

TOWARDS MULTIFUNCTIONAL COMPOSITES BY CARBON NANOTUBES-BASED NANO/MICRO HYBRID STRUCTURES

Delong He¹ and Jinbo Bai²

^{1, 2} Laboratoire de Mécanique des Sols, Structures et Matériaux, UMR 8579 CNRS, Ecole CentraleSupélec, Université Paris-Saclay, Grande Voie des Vignes, 92290, Chatenay-Malabry, France

¹delong.he@centralesupelec.fr & ²jinbo.bai@centralesupelec.fr; ^{1, 2}<http://www.centralesupelec.fr/>

Keywords: Carbon Nanotubes, hybrid structures, Interface/Interphase, Multifunctional composites

ABSTRACT

Polymer composites with enhanced mechanical and functional properties are highly desired to develop light-weight function-integrated structures and devices. In this communication, we summarize some of our recent works concerning the development of multifunctional composites through nano/micro hybrid structures which consist of carbon nanotubes (CNTs) and microparticles or long fibers. A variety of CNTs-based hybrid structures were realized by an in-situ chemical vapor deposition (CVD) using different micrometer substrates such as ceramic particles (Al₂O₃, SiC, BaTiO₃...), graphite nanoplates and continuous fibers. The nanotube organisation state, aspect ratio, areal number density can be modulated by varying the CVD parameters, such as temperature, carbon source and hydrogen ratio. The hierarchical multifunctional composites were also prepared with the as-developed nano/micro hybrids. It was found that the interfacial/interphase properties between polymer matrix and microscopic reinforcement are greatly changed due to CNT grafting and modified interfacial area and interphase volume and property. The improved composite properties including mechanical, electrical and dielectric properties have been obtained due to ameliorated CNT dispersion and their arrangement in polymer matrix. The hybridization between CNTs and microparticles or long fibers shows huge potential to cost-effectively realize large-scale application of CNTs in the fields of structure health monitoring, electromagnetic shielding and absorption, lightning strike protection, de-icing, etc.

1 INTRODUCTION

Advanced polymer composites play increasingly important roles in the fields ranging from microelectronics to aeronautics and aerospace, automotive and new energy, due to their light weight and excellent properties [1, 2] [3, 4]. Nowadays it is still highly desired to continuously improve their damage resistance and functional properties to meet higher structure performance requirements while reducing structure weight and CO₂ emission. A significant improvement of multifunctional properties of the composites has been reported by incorporating carbon nanotubes (CNTs) or graphene, due to their specific structures and extraordinary properties [5-7]. For example, the addition of CNTs has been considered as one of the most promising solutions to realize electrically conductive GFRPs with adjustable high conductivity while retaining their intrinsic structural properties [8, 9] [10-13]. Moreover, these GFRPs have also been demonstrated to have potential applications in structural health monitoring, electromagnetic absorption and shielding, in-situ cure monitoring, thermal energy harvesting [14-18].

However, the strong agglomeration tendency of these nanomaterials makes them particularly difficult to produce defect-free composites, resulting in mechanical property deterioration and much lower reinforcing effects than the expected values. Meanwhile, the addition of CNTs unavoidably causes resin viscosity increase, and deteriorates the ease of processing [19, 20]. Thus, it is still a tough but attractive research topic to cost-efficiently integrate functional properties while retaining their intrinsic structural performance of advanced polymer composites.

A number of methods have been developed to improve CNT dispersion in polymer matrix. Surface functionalization is one of the commonly used approaches whose principle is to attach chemical groups or molecules on CNT sidewall or ends using a chemical, physical or electrochemical way [21, 22]. The covalent functionalization unavoidably generates π conjugation disruption, sidewall defects and shortening of nanotubes, and significantly impacts the composite mechanical properties and more profoundly their thermal and electrical properties. The non-covalent ways such as polymer wrapping and surfactants, based on van der Waals forces or π - π stacking, are still limited due to the low thermal stability and weak mechanical performance of surfactants, compatibility, etc. Thus, a compromise between good dispersion and property deterioration is generally made for the available CNTs-contained composites.

CNT hybridization with microscopic materials provides an attractive way to integrate functional properties in conventional particle and fiber reinforced structural composites. The hybrid structures consisting of CNTs grafting on microparticles are expected to take good advantage of nano and micro synergistic reinforcements [23, 24]. The organized hybrid structures favor the control over CNT alignment in the composites. They could be synthesized by in-situ growing CNTs on various micrometer materials, such as ceramic particles (Al_2O_3 , SiC, BaTiO_3 , TiO_2 , etc.), graphene nanoplatelets (GNPs), and fibers (carbon, alumina, glass, etc.) [25] [26-31]. Also, some studies show that the hybrids-reinforced nanocomposites have the improved mechanical and multifunctional properties, compared to a random mixture of CNTs and microparticles [30, 32]. It is well known that CNT growth and self-organization on the microparticles depend greatly on the substrate crystallization structure and morphologies, as well as CVD conditions used [26, 29, 33]. In most cases reported, the CNTs bundles (agglomerated) have been found, especially for long CNTs, which may generate structural defects in composites. Therefore, it is highly desired to have one kind of hybrid structure with well-dispersed but aligned CNTs in order to explore to a great extent their hybrid reinforcing role in mechanical and functional properties.

In this communication, we summarize some of our recent works [34, 35] concerning the development of multifunctional composites through CNTs-based hybrid structures. Two kinds of hybrids, CNTs-microparticles (CNTs- $\mu\text{Al}_2\text{O}_3$) and CNTs-Glass fibers (CNTs-GF) are taken as examples. Their in-situ synthesis and the corresponding hierarchical composites were manufactured by following the optimized procedures. Detailed investigation on the mechanical, electrical and dielectric properties of the composites was conducted to evaluate the reinforcing roles of the hybrid structures. The interfacial/interphase properties between polymer matrix and microscopic reinforcement are given a particular attention.

2 EXPERIMENTAL

2.1 Hybrid structure synthesis

The synthesis of the CNTs-based hybrids was carried out by CVD in a quartz tube which was heated by an electrical resistance furnace (CARBOLITE®), as reported in reference [34, 35]. The substrates such as $\mu\text{Al}_2\text{O}_3$ particles of 1-10 μm in diameter or glass fiber tissue were supported on a quartz plate (30 mm in width \times 500 mm in length) placed in the center of tube, and heated in the presence of a gas mixture of argon and hydrogen. The synthesis temperature varied from 550 $^\circ\text{C}$ – 800 $^\circ\text{C}$, depending on the type of substrate and the CNT structures desired. A xylene (ACS, 98.5%, Alfa Aesar) solution dissolved with 0.01-0.1 g ml^{-1} ferrocene (ACS, 99% Powder, Alfa Aesar) was injected at a speed of 12-24 ml h^{-1} into the reactor by a syringe injector in form of spray. The sprayed solution was carried into the reaction zone by the carrier gases. Herein, the ferrocene was served as catalyst precursor. At the same time, the second carbon source-acetylene was also fed at a flow rate of 0.05-0.3 L min^{-1} . After the synthesis, the furnace was cooled down to room temperature under argon protective atmosphere (1 L min^{-1}).

2.2 Composite preparation

CNTs- $\mu\text{Al}_2\text{O}_3$ hybrids/Epoxy composites: The polymer matrix used in this study is epoxy resin (1080S, Resoltech Ltd., France) with curing agent (1084, Resoltech Ltd.). The as-synthesized urchin-

like CNTs- $\mu\text{Al}_2\text{O}_3$ hybrids were manually mixed with epoxy resin. Then, the mixtures were further dispersed using a three-roll mill (EXAKT 80, Germany), following a preparation protocol. The curing agent was added to the collected suspension at mass ratio of 1/3 to the epoxy resin, and then manually mixed to obtain a homogeneous suspension. The resulting mixture was firstly degassed for 30 min at room temperature in a vacuum oven, and then poured into an aluminum mold with dumbbell-shape and square, which was then fasten with 4 screw bolts. The composites were obtained after being cured at 60 °C for 15 h. Dumbbell-shape samples with 1 mm in thickness, 50 mm in length and 4 mm in gage width were obtained and edge-polished for tensile testing according to ASTM D638. The samples with dimension about 10 mm \times 10 mm \times 1 mm were achieved for dielectric property, ac conductivity and thermal conductivity measurements.

CNTs-GF hybrids/Epoxy composites: The 1080S/1084 (100:33 in weight) resin mixture was first mechanically stirred for 10 min, and then degassed at room temperature for 30 min in a vacuum oven. The obtained mixture was uniformly spread over each GF or CNT-GF tissue until the latter was completely immersed. The six plies of GF or CNT-GF tissue were layered-up by hand along the same wrap orientation, and put into a vacuum bag which maintained a constant pressure of - 0.5 bar by a mechanical pump. The curing process was conducted using a hot press. The temperature was first heated up to 60 °C at a rate of 2 °C min⁻¹ under -0.5 bar, and then hold for 2 hours under 0.7 MP. Then, the airbag was quickly moved into an oven preheated to 60 °C for another 15 hours under atmosphere condition. The as-prepared laminates were cut into different sizes for further microstructure characterizations and property tests.

2.3 Characterizations

Thermogravimetric analysis (TGA) was carried out using a thermal analyser (NETZSCH STA 449 F3), under a mixed atmosphere of oxygen and nitrogen with a flow rate of 20: 20 ml min⁻¹, respectively. The analysed temperature range was from room temperature to 900 °C with a heating rate of 10 °C min⁻¹.

Microstructure characterization of the hybrids and the composites was conducted using a scanning electron microscope (SEM, LEO 1530 Gemini) and a transmission electron microscope (TEM, JEOL 1200 EX, and TITAN³ G2), as well as a Raman spectroscopy (Jobin Yvon).

The AC conductivity and dielectric properties including dielectric permittivity (ϵ') and loss tangent ($\tan \delta$) of the composites were measured using an impedance/gain-phase analyzer (Solatron 1260) with the frequency range from 10² to 10⁷ Hz at 1 Volt at room temperature. The in-plane and through-plane electrical conductivities of as-prepared CNTs-GF/epoxy composites were measured using a voltage-current meter (Keithley 2400) using a two-probe method. The sample size used was about 10 mm (length) \times 10 mm (width) \times 1 mm (thickness).

The thermo-mechanical properties of the GFRP composites were also investigated by dynamic mechanical analysis (DMA, NETZSCH 242C) under three-point-bending mode. The characterizations were carried out at a frequency of 1 Hz, and the temperature was varied from 30 to 200 °C at a heating rate of 3 °C min⁻¹. The span length used was 40 mm, and the sample size was 60 mm in length and 11 mm in width.

The tensile tests of the dumbbell-shaped composite samples were carried out with a machine (Instron 5544 with a 2 kN load cell) at a fixed displacement rate of 0.2 mm min⁻¹. The flexural properties of GFRPs were measured under three-point bending mode at a span length of 25.4 mm and a cross head speed of 1 mm min⁻¹, according to ASTM D2344 standard. The sample size used was around 60 mm \times 12.7 mm \times 1 mm.

Single fiber tensile test, single bundle test and single fiber fragmentation test were carried out using the instrument-Instron 5544 with a load cell of 5N and 2 kN, respectively. The single fiber tensile test was conducted according to NF ISO 11566. The cross-head speed used was 0.5 mm min⁻¹ and the gauge length was about 25 mm. The single fiber bundle tensile tests were done at the same cross-head displacement speed, using a gauge length of 50 mm.

3 RESULTS AND DISCUSSION

3.1 In situ CVD synthesis of Nano/micro hybrids

Divers multi-scale hybrids can be synthesized by in situ grafting CNTs on micrometer materials. As shown in Fig. 1, we have successfully developed various hybrid structures with the various micrometer materials such as ceramic particles (Al_2O_3 , SiC, BaTiO_3 , TiO_2 ...), graphite nanoplates, and a variety of fibers [26-31]. It was noticed that the growth of CNTs followed a bottom-up growth model. Under the experimental conditions used, ferrocene can be efficiently decomposed by releasing active iron atoms for iron nanoparticle nucleation and growth on the substrates. The catalyst particles accelerate the decomposition of hydrocarbons which feed highly efficient carbon sources for CNT growth.

The nanotube organization state, aspect ratio, areal number density can be modulated by varying the CVD parameters, such as temperature, carbon source and hydrogen ratio [36]. For example, the self-organization of CNTs on microparticles allowed producing various distinguished hybrid structures, such as “short-dense-homogeneous”, “six-branch” and “urchin-like” on spherical alumina microparticles. The involved growth mechanisms were also investigated in detail: (1) multiple physicochemical phenomena in gas atmosphere, (2) microparticle crystallography, and (3) nanotube interaction due to Van der Waals’s force.

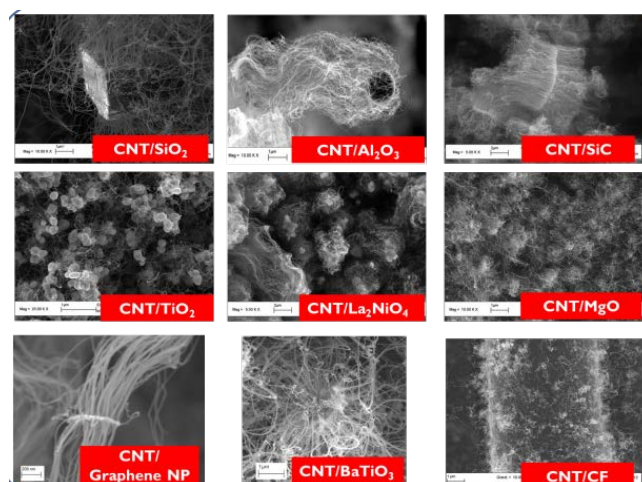


Figure 1: SEM images of divers CNTs-based hybrid structures synthesized by in-situ CVD method

3.2 CNTs-microparticle hybrids and reinforced polymer composites

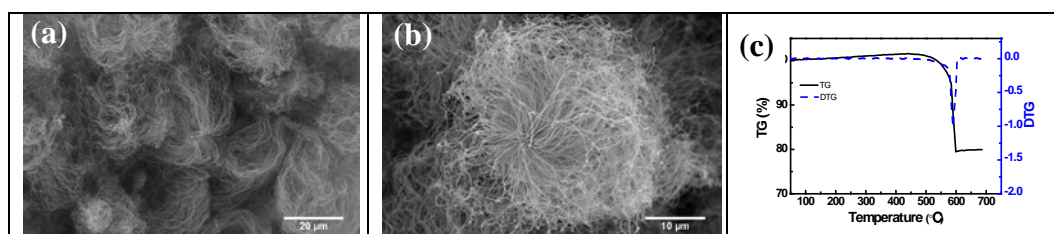


Figure 2: SEM images of the urchin-like hybrid structures consisting of multi-walled carbon nanotubes and alumina microspheres: (a) low and (b) high magnification. (c) TG and DTG curves of the as-produced urchin-like CNTs/ Al_2O_3 hybrids.

Take CNTs- $\mu\text{Al}_2\text{O}_3$ as an example, as shown in Fig. 2a and b. The synthesized nanotubes are almost individually distributed on $\mu\text{Al}_2\text{O}_3$ surface. The surrounded rigid nanotubes and microspherical alumina core form an urchin-like hybrid structure. The CNTs have an average diameter ~ 50 nm and an average length about $40 \mu\text{m}$, corresponding to a growth rate about $2.5 \mu\text{m min}^{-1}$. Fig. 2c shows the TGA curve of the CNTs- $\mu\text{Al}_2\text{O}_3$ hybrids. It can be found that the nanotubes were thermally stable up

to 500 °C under oxygen and nitrogen atmosphere, and the weight loss occurred between 500 and 600 °C due to CNT oxidation. The maximum decomposition temperature was observed at 590 °C (as indicated by DTG curve) under the measured condition used. The residual mass above 600 °C corresponds to the one of alumina microparticles. The CNTs weight ratio in the as-synthesized urchin-like hybrids was about 20 wt.%.

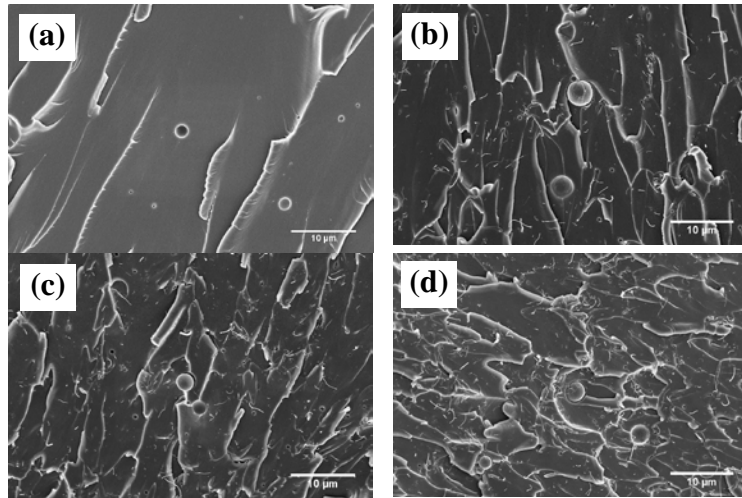


Figure 3: SEM images of the cross-section of pure epoxy (a) and those of the composites with varied mass fractions of the hybrids: (b) 0.5 %, (c) 1.5 % and (d) 2.5 %.

Figure 3 shows SEM images of the cross sections of the composites with varied mass fractions of the hybrids. No agglomeration of hybrid particles is found, and CNTs are well dispersed in the epoxy matrix. Meanwhile, it can be seen that CNTs are around $\mu\text{Al}_2\text{O}_3$ zone, and some of them attach on the alumina surface, and others have detached. Obviously, the increased number of CNTs ends emerges from the matrix with the increase of the hybrid volume fraction in the composite.

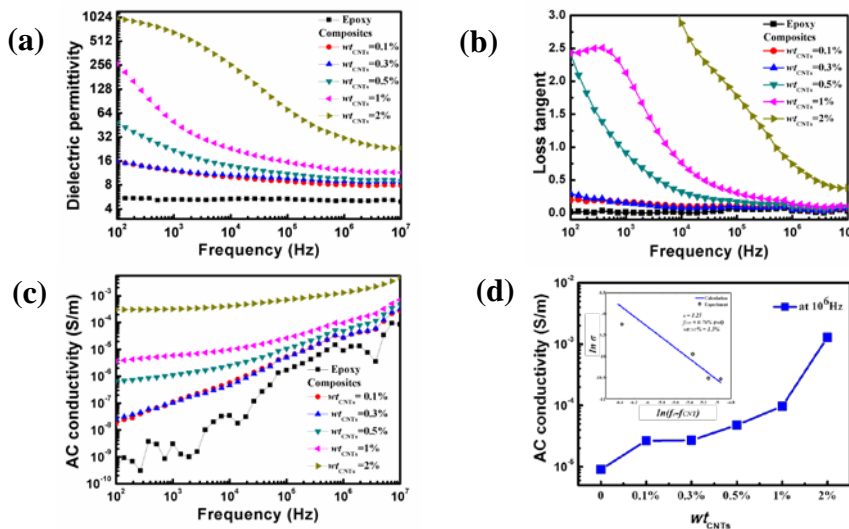


Figure 4: Frequency dependence of the dielectric properties of the composites with varied wt_{CNTs} from 10^2 to 10^7 Hz: (a) dielectric permittivity, (b) loss tangent and (c) AC conductivity. (d) AC conductivity at 10^6 Hz and the inset graph is the best liner fitting according to percolation threshold theory.

The room temperature dielectric permittivity (ϵ'), loss tangent ($\tan \delta$) and AC conductivity of the urchin-like hybrid reinforced composites from 10^2 to 10^7 Hz are shown in Fig.4a-c. First, the dielectric properties of the composites with different $wt_{CNTs-\mu\text{Al}_2\text{O}_3}$ show strong frequency and weight fraction

dependence especially at low frequency range (10^2 - 10^4 Hz). There is a dramatic increase happening in both ϵ' and $\tan \delta$ when the fraction wt_{CNTs} is close to 1 %. This can be explained by classical percolation theory [37, 38]. In our system, when CNTs weight fraction is low (less than 1%), epoxy layers isolate the conductive CNTs and the network of micro-capacitors fails to form, which makes ϵ' at the low level. However, when wt_{CNTs} approaches to the critical value (percolation threshold), each micro-capacitor will be correlated with the significant increase in the intensity of the local electric field. This usually generates surface plasma resonance or charge injection at the CNT-epoxy matrix interfaces which promotes the migration and accumulation of the charge carriers and consequently cause the interfacial polarization. We use the linear fit of AC conductivity to get the percolation threshold for the composites by the power law:

$$\sigma_c \propto \sigma_f (f_c - f)^s \quad (1)$$

where σ_c and σ_f are the conductivities of composites and conductive fillers, respectively; f and f_c are the volume fraction of the fillers and the percolation threshold, respectively; s is the dimensionality-dependent critical exponent.

The result of linear fitting for the composite σ_c is shown in Fig. 4d and the best linear fit gives $s = 1.25$ which agrees with the universal one (in the range from 0.7 to 1.3) [37]. The percolation threshold f_c is 0.76 %, corresponding $wt_{CNTs} = 1.3$ %, calculated by CNT volume fraction according to the experimental data. Compared with common CNT reinforced epoxy composites, f_c in our system is really small. This may be attributed to the special structure of urchin-like hybrids which improve the homogeneous dispersion of CNTs in epoxy matrix, avoiding CNT's agglomeration. Besides, this structure may also conversely prevent the restacking of μAl_2O_3 particles and create more area of interfaces in the composites and thus enhance the synergistic effect of μAl_2O_3 and epoxy.

The frequency dependence of AC conductivity in Fig. 4c is also provided evidence for the evolution for CNT's network. It is could be found that the AC conductivity of the composite increases both with the $wt_{CNTs-\mu Al_2O_3}$ and the frequency when the hybrid's content at a low level. Meanwhile, the effect of CNTs- μAl_2O_3 reinforcement on the composite conductivity becomes less evident with the increase of the frequency. However, a huge improvement is seen when the $wt_{CNTs-\mu Al_2O_3}$ is beyond 2.5 wt%. When $wt_{CNTs-\mu Al_2O_3}$ is 10%, the composite conductivity becomes frequency independent and shows a conductive behaviour. This indicates that the CNT conductive network is gradually constructed when the hybrid mass fraction is beyond 2.5 wt. %.

The tensile properties of the composites were measured in order to evaluate the influence of hybrid addition on the composite mechanical properties. It is found that the composite Young's modulus increases with the CNTs- μAl_2O_3 mass fraction. The E_{comp} varies from 2.1 GPa to 2.7 GPa when the $wt_{CNTs-\mu Al_2O_3}$ evolves from 0.005 to 0.1. As compared to pure epoxy ($E = 2.1$ GPa), an improvement as high as 26 % was obtained when the $wt_{CNTs-\mu Al_2O_3}$ was 0.1. A widely used Halpin-Tsai model [39, 40] is employed in order to model the reinforcing roles of the urchin-like hybrid structures on the Young's modulus of the composites, by taking into account of both the detached nanotubes and the ones attached on the microparticles. The modeled results correspond with the experimental data much better than the ones obtained by using the integral hybrid structure or the wholly random distribution states. That explains that the alignment of CNTs due to urchin-like hybrid is more efficient in reinforcing polymer composites than random distribution.

3.3 CNTs-fiber hybrids and reinforced polymer composites

Take CNTs-GFs as an example as shown in Fig. 5a, the color of as-received white GF tissue turned to black after growth of 2 wt. % CNTs. SEM image shows that nanotubes grew perpendicularly and homogeneously on the whole surface of fabric and on each fiber (Fig. 5b). More importantly, each GF was cover by a continuous cylindrical shell consisting of aligned nanotubes. TEM images (Fig. 5c-d) furthermore conform that as-synthesized CNTs did grow in an aligned way, and each nanotube was perpendicular to the GF surface with a length of around 2.5 μm at $wt_{CNT} = 2$ %, instead of entangling together in a random way. The diameter of synthesized CNTs was between 10 and 20 nm. This kind of well-aligned organization of nanotubes favors polymer resin diffusion by capillary force during composite fabrication [41, 42].

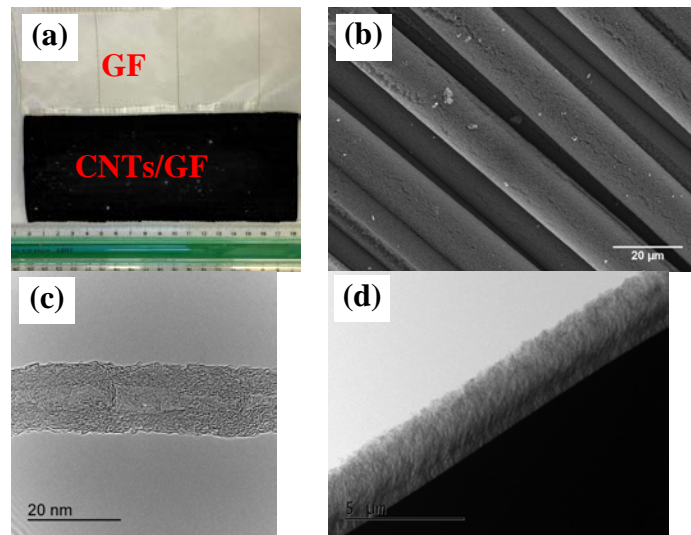


Figure 5. (a) Images of pristine GF tissue and the one after growth of 2 wt .% CNTs; (b) low magnification SEM images of CNTs/GF tissue, and (c) high and (d) low resolution TEM images of one nanotube and one CNTs-GF hybrid, respectively.

The electrical conductivity of the CNTs-GF/Epoxy composites is demonstrated in Fig. 6a. It can be seen that both the in-plane and through-plane electrical conductivities increased with the increase of the mass fraction of CNTs grown on the GF fabrics. The through-plane electrical conductivity was increased from 5E-09 S/m to 3.5 S/m when wt_{CNT} varied from 0 to 7 %. Meanwhile, the in-plane one was increased from 5E-07 S/m to 100 S/m when wt_{CNT} varied from 0 to 7 %. It was also found that the in-plane and through-plane electrical conductivity increased simultaneously with wt_{CNT} , following a similar variation rule. As shown in Fig. 6b, a sharp improvement of the conductivities is observed when wt_{CNT} is more than 0.5 %. Moreover, the dielectric property measurements showed the composites behaved as dielectric materials at $wt_{CNT} = 0.2$ %, but a significant increase on both the dielectric constant and loss tangent was observed at $wt_{CNT} = 0.5$ %. This indicates that continuously conductive pathways are formed in both through-thickness and in-plane directions. Therefore, the growth of CNTs on GF cloth allows modulating the composite electrical conductivity at a very wide range from nearly isolating to high dielectric, and then to highly conductive ones. This is highly desired to design composite properties such as dielectric constant or conductivity according to real service requirements.

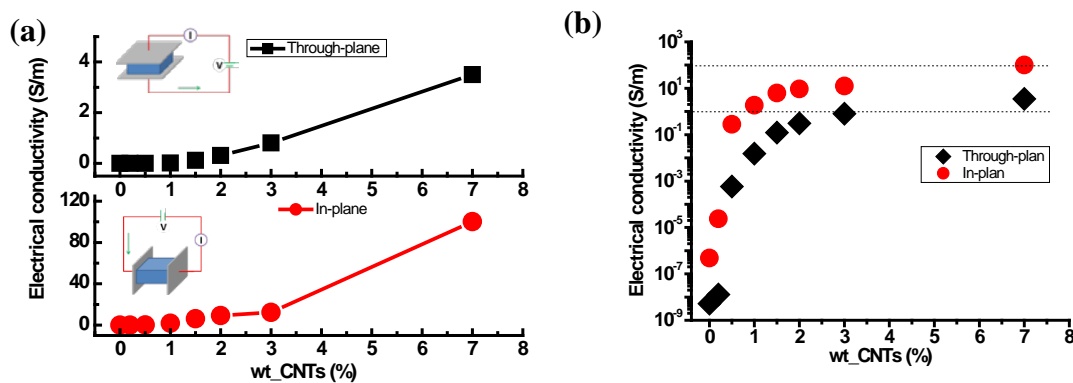


Figure 6. In-plane and through-plane electrical conductivities of the composites as a function of the mass fraction of CNTs in-situ growing on the surface of GF fabric surface.

The microstructures of the CNTs-GF/Epoxy composites were characterized by SEM in order to understand their electrically conductive behaviors and related mechanism. The cross-sections of the composites with varied CNT fractions after breaking in liquid nitrogen are demonstrated in Fig. 7. First, few visible defects such as pores and CNT aggregates are presented in the structures, indicating that the composites have good quality. It also indicates that the growth of CNTs on GF tissue can adapt well with currently widely used composite production techniques, without introducing evident defects. Comparing with the commonly used dispersion way which may cause significant increase of matrix resin viscosity [43], in-situ growth of CNTs on the fabrics provides a highly efficient way to introduce CNTs, even high mass fractions, into structural composites. This advantage is highly appreciated by industrial sectors for their potential large-scale applications. Second, a distinguished annular region is obviously observed around each GF by SEM, when CNT mass fraction is higher than 0.5 %. This region bridges together GF and matrix bulk, forming a distinguished interphase which has the properties different from bulk matrix. It is well known that interfacial and interphase properties take a determining role in realizing high performance fiber and polymer composites [44]. The introduction of CNTs could reinforce the interphase region [45]. In our case, CNT volume concentration in annular interphase zones is higher than that in other parts of bulk matrix, and the CNT alignment on GF in the composites was conserved from the as-synthesized CNTs-GF. Similarly, the interphase region thickness increases progressively with the mass fraction and shell thickness of CNTs grown on GFs. As a result, at higher w_{CNT} the interconnection between adjacent interphase regions generates increased electrical conduction pathway numbers, thus displays greatly increased electrical conductivity.

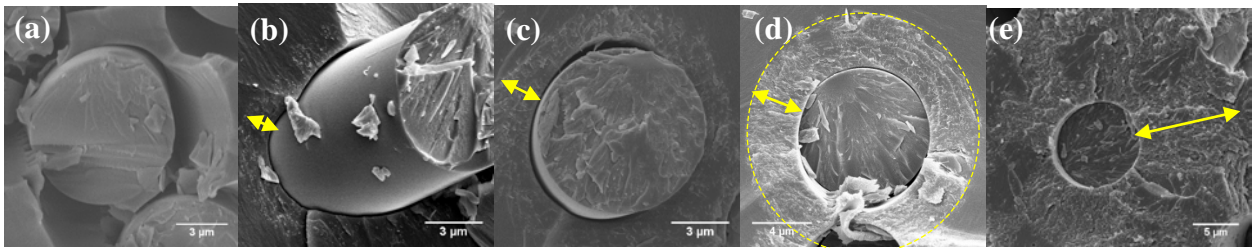


Figure 7. SEM images of interface/interphase in GF/Epoxy composite (a), and the annular ones (indicated by arrows) consisting of aligned nanotubes around glass fiber in CNTs-GF/Epoxy composites: (b) $w_{\text{CNT}}=0.5\%$, (c) $w_{\text{CNT}}=1.5\%$, (d) $w_{\text{CNT}}=3\%$ and (e) $w_{\text{CNT}}=7\%$.

As we know, there are multiple interfaces included in the hierarchical CNTs-GF composites: CNTs/GF, CNTs/matrix and GF/matrix one. Thus, the interfacial shear strength (IFSS) of CNTs-GF in the composites is a general result of the interaction of these three interfaces. The single fiber and fiber bundle tensile tests also demonstrated that the influence of CVD procedure and CNT grafting on the mechanical properties of glass fiber is negligible under the conditions that we studied. Furthermore, the single fiber fragmentation tests show that the grafting of CNTs on GF may improve the interfacial properties between GF and matrix.

4 CONCLUSIONS

In summary, in-situ growth of CNTs on microparticles and long fiber tissue can be achieved by a one-step CVD, and the grafted CNTs homogeneously and perpendicularly aligned on the surface of each fiber, forming one dimensional “core-shell” structure. We demonstrated that the CNT mass fraction and length could be modulated in a controlled way by varying the CVD conditions. The hierarchical CNTs- $\mu\text{Al}_2\text{O}_3$ and CNTs-GF were used to produce multifunctional structural composites. The electrical conductivities of as-produced composites greatly increased as a function of the weight fraction of CNTs grafted on the GF tissue, for example, as high as 100 S/m at $w_{\text{CNT}}=7\%$ for CNTs-GF composites. The studies on the thermo-mechanical and flexural properties demonstrated the CNTs-GF/Epoxy composites exhibited the improved structural properties, with retention of 100 % of their original thermal stability. The multifunctional properties of the CNTs- $\mu\text{Al}_2\text{O}_3$ /epoxy and CNTs-GF

composites are mainly due to the specific CNT arrangement and multiscale reinforcing effects. Thus, the CNTs-based hybrid structures endow conventional polymers with excellent multifunctional properties, while improving their original structural properties. Besides, the ease of scaled-up CVD production makes the hybrids and their composites promising to be widely applied in various fields from electronics to aeronautics and aerospace.

REFERENCES

- [1] C. Soutis, "Fibre reinforced composites in aircraft construction," *Progress in Aerospace Sciences*, vol. 41, pp. 143-151, Feb 2005.
- [2] J. M. Thomassin, C. Jerome, T. Pardoën, C. Bailly, I. Huynen, and C. Detrembleur, "Polymer/carbon based composites as electromagnetic interference (EMI) shielding materials," *Materials Science & Engineering R-Reports*, vol. 74, pp. 211-232, Jul 2013.
- [3] P. K. Mallick, *Fiber-Reinforced Composites: Materials, Manufacturing, and Design, Second Edition*: Taylor & Francis, 1993.
- [4] B. Harris, *ENGINEERING COMPOSITE MATERIALS* London: The Institute of Materials, 1999.
- [5] Z. Spitalsky, D. Tasis, K. Papagelis, and C. Galiotis, "Carbon nanotube-polymer composites: Chemistry, processing, mechanical and electrical properties," *Progress in Polymer Science*, vol. 35, pp. 357-401, Mar 2010.
- [6] M. F. L. De Volder, S. H. Tawfick, R. H. Baughman, and A. J. Hart, "Carbon Nanotubes: Present and Future Commercial Applications," *Science*, vol. 339, pp. 535-539, Feb 2013.
- [7] M. F. L. D. Volder, S. H. Tawfick, R. H. Baughman, and A. J. Hart, "Carbon Nanotubes: Present and Future Commercial Applications," *SCIENCE*, vol. 339 pp. 535-539, 2013.
- [8] S.-I. Gao, R.-C. Zhuang, J. Zhang, J.-W. Liu, and E. Mäder, "- Glass Fibers with Carbon Nanotube Networks as Multifunctional Sensors," vol. - 20, pp. - 1893, 2010.
- [9] M. H. G. Wichmann, J. Sumfleth, F. H. Gojny, M. Quaresimin, B. Fiedler, and K. Schulte, "Glass-fibre-reinforced composites with enhanced mechanical and electrical properties - Benefits and limitations of a nanoparticle modified matrix," *Engineering Fracture Mechanics*, vol. 73, pp. 2346-2359, Nov 2006.
- [10] L. Boeger, M. H. G. Wichmann, L. O. Meyer, and K. Schulte, "Load and health monitoring in glass fibre reinforced composites with an electrically conductive nanocomposite epoxy matrix," *Composites Science and Technology*, vol. 68, pp. 1886-1894, Jun 2008.
- [11] C. S. Grimmer and C. K. H. Dharan, "High-cycle fatigue of hybrid carbon nanotube/glass fiber/polymer composites," *Journal of Materials Science*, vol. 43, pp. 4487-4492, 2008// 2008.
- [12] L. Liao, X. Wang, P. Fang, K. M. Liew, and C. Pan, "Interface Enhancement of Glass Fiber Reinforced Vinyl Ester Composites with Flame-Synthesized Carbon Nanotubes and Its Enhancing Mechanism," *ACS Applied Materials & Interfaces*, vol. 3, pp. 534-538, 2011/02/23 2011.
- [13] A. Warriar, A. Godara, O. Rochez, L. Mezzo, F. Luizi, L. Gorbatikh, *et al.*, "The effect of adding carbon nanotubes to glass/epoxy composites in the fibre sizing and/or the matrix," *Composites Part A: Applied Science and Manufacturing*, vol. 41, pp. 532-538, 4// 2010.
- [14] A. Y. Boroujeni, M. Tehrani, M. Manteghi, Z. Zhou, and M. Al-Haik, "Electromagnetic Shielding Effectiveness of a Hybrid Carbon Nanotube/Glass Fiber Reinforced Polymer Composite," *Journal of Engineering Materials and Technology*, vol. 138, pp. 041001-041001, 2016.
- [15] J. Sebastian, N. Schehl, M. Bouchard, M. Boehle, L. Li, A. Lagounov, *et al.*, "Health monitoring of structural composites with embedded carbon nanotube coated glass fiber sensors," *Carbon*, vol. 66, pp. 191-200, 1// 2014.
- [16] S. E. Lee, W. J. Lee, K. S. Oh, and C. G. Kim, "Broadband all fiber-reinforced composite radar absorbing structure integrated by inductive frequency selective carbon fiber fabric and carbon-nanotube-loaded glass fabrics," *Carbon*, vol. 107, pp. 564-572, Oct 2016.

- [17] B. Hao, Q. Ma, S. D. Yang, E. Mader, and P. C. Ma, "Comparative study on monitoring structural damage in fiber-reinforced polymers using glass fibers with carbon nanotubes and graphene coating," *Composites Science and Technology*, vol. 129, pp. 38-45, Jun 2016.
- [18] J. Zhang, R. Zhuang, J. Liu, E. Mäder, G. Heinrich, and S. Gao, "Functional interphases with multi-walled carbon nanotubes in glass fibre/epoxy composites," *Carbon*, vol. 48, pp. 2273-2281, 7// 2010.
- [19] F. H. Gojny, M. H. G. Wichmann, B. Fiedler, W. Bauhofer, and K. Schulte, "Influence of nano-modification on the mechanical and electrical properties of conventional fibre-reinforced composites," *Composites Part A: Applied Science and Manufacturing*, vol. 36, pp. 1525-1535, 11// 2005.
- [20] Z. Fan, M. H. Santare, and S. G. Advani, "Interlaminar shear strength of glass fiber reinforced epoxy composites enhanced with multi-walled carbon nanotubes," *Composites Part A: Applied Science and Manufacturing*, vol. 39, pp. 540-554, 3// 2008.
- [21] K. Balasubramanian and M. Burghard, "Chemically functionalized carbon nanotubes," *Small*, vol. 1, pp. 180-192, Feb 2005.
- [22] M. Moniruzzaman and K. I. Winey, "Polymer nanocomposites containing carbon nanotubes," *Macromolecules*, vol. 39, pp. 5194-5205, Aug 2006.
- [23] L. J. Ci and J. B. Bai, "Novel micro/nanoscale hybrid reinforcement: Multiwalled carbon nanotubes on SiC particles," *Advanced Materials*, vol. 16, pp. 2021-+, Nov 2004.
- [24] E. T. Thostenson, C. Li, and T.-W. Chou, "Nanocomposites in context," *Composites Science and Technology*, vol. 65, pp. 491-516, 3// 2005.
- [25] A. Rahaman and K. K. Kar, "Carbon nanomaterials grown on E-glass fibers and their application in composite," *Composites Science and Technology*, vol. 101, pp. 1-10, Sep 2014.
- [26] D. He, M. Bozlar, M. Genestoux, and J. Bai, "Diameter- and length-dependent self-organizations of multi-walled carbon nanotubes on spherical alumina microparticles," *Carbon*, vol. 48, pp. 1159-1170, 4// 2010.
- [27] D. He, H. Li, W. Li, P. Haghi-Ashtiani, P. Lejay, and J. Bai, "Growth of carbon nanotubes in six orthogonal directions on spherical alumina microparticles," *Carbon*, vol. 49, pp. 2273-2286, 6// 2011.
- [28] D. He, H. Li, and J. Bai, "Experimental and numerical investigation of the position-dependent growth of carbon nanotube–alumina microparticle hybrid structures in a horizontal CVD reactor," *Carbon*, vol. 49, pp. 5359-5372, 12// 2011.
- [29] W. Li, J. Yuan, Y. Lin, S. Yao, Z. Ren, H. Wang, *et al.*, "The controlled formation of hybrid structures of multi-walled carbon nanotubes on SiC plate-like particles and their synergetic effect as a filler in poly(vinylidene fluoride) based composites," *Carbon*, vol. 51, pp. 355-364, 1// 2013.
- [30] W. Li, A. Dichiara, and J. Bai, "Carbon nanotube–graphene nanoplatelet hybrids as high-performance multifunctional reinforcements in epoxy composites," *Composites Science and Technology*, vol. 74, pp. 221-227, 1/24/ 2013.
- [31] B. Fan, F. Bedoui, S. Weigand, and J. Bai, "Conductive Network and β Polymorph Content Evolution Caused by Thermal Treatment in Carbon Nanotubes-BaTiO₃ Hybrids Reinforced Polyvinylidene Fluoride Composites," *The Journal of Physical Chemistry C*, vol. 120, pp. 9511-9519, 2016/05/05 2016.
- [32] M. Bozlar, D. L. He, J. B. Bai, Y. Chalopin, N. Mingo, and S. Volz, "Carbon Nanotube Microarchitectures for Enhanced Thermal Conduction at Ultra low Mass Fraction in Polymer Composites," *Advanced Materials*, vol. 22, pp. 1654-+, Apr 2010.
- [33] D. He and J. Bai, "Acetylene-Enhanced Growth of Carbon Nanotubes on Ceramic Microparticles for Multi-Scale Hybrid Structures," *Chemical Vapor Deposition*, vol. 17, pp. 98-106, Jun 2011.
- [34] D. He, B. Fan, H. Zhao, M. Yang, H. Wang, J. Bai, *et al.*, "Multifunctional polymer composites reinforced by carbon nanotubes–Alumina hybrids with urchin-like structure," *Materials Today Communications*, vol. 11, pp. 94-102, 6// 2017.

- [35] D. He, B. Fan, H. Zhao, X. Lu, M. Yang, Y. Liu, *et al.*, "Design of Electrically Conductive Structural Composites by Modulating Aligned CVD-Grown Carbon Nanotube Length on Glass Fibers," *ACS Applied Materials & Interfaces*, vol. 9, pp. 2948-2958, 2017/01/25 2017.
- [36] D. He, M. Bozlar, M. Genestoux, and J. Bai, "Diameter-and length-dependent self-organizations of multi-walled carbon nanotubes on spherical alumina microparticles," *Carbon*, vol. 48, pp. 1159--1170, 2010.
- [37] C. W. Nan, Y. Shen, and J. Ma, "Physical Properties of Composites Near Percolation," in *Annual Review of Materials Research, Vol 40*. vol. 40, D. R. Clarke, M. Ruhle, and F. Zok, Eds., ed Palo Alto: Annual Reviews, 2010, pp. 131-151.
- [38] Z. M. Dang, J. K. Yuan, S. H. Yao, and R. J. Liao, "Flexible Nanodielectric Materials with High Permittivity for Power Energy Storage," *Advanced Materials*, vol. 25, pp. 6334-6365, Nov 2013.
- [39] J. N. Coleman, U. Khan, W. J. Blau, and Y. K. Gun'ko, "Small but strong: A review of the mechanical properties of carbon nanotube-polymer composites," *Carbon*, vol. 44, pp. 1624-1652, 8// 2006.
- [40] T. T. Erik and C. Tsu-Wei, "On the elastic properties of carbon nanotube-based composites: modelling and characterization," *Journal of Physics D: Applied Physics*, vol. 36, p. 573, 2003.
- [41] M. De Volder, S. H. Tawfick, S. J. Park, D. Copic, Z. Zhao, W. Lu, *et al.*, "Diverse 3D Microarchitectures Made by Capillary Forming of Carbon Nanotubes," *Advanced Materials*, vol. 22, pp. 4384-4389, 2010.
- [42] X. Wang, Z. Z. Yong, Q. W. Li, P. D. Bradford, W. Liu, D. S. Tucker, *et al.*, "Ultrastrong, Stiff and Multifunctional Carbon Nanotube Composites," *Materials Research Letters*, vol. 1, pp. 19-25, 2013/03/01 2013.
- [43] S. S. Rahatekar, K. K. K. Koziol, S. A. Butler, J. A. Elliott, M. S. P. Shaffer, M. R. Mackley, *et al.*, "Optical microstructure and viscosity enhancement for an epoxy resin matrix containing multiwall carbon nanotubes," *Journal of Rheology*, vol. 50, pp. 599-610, 2006.
- [44] X. Zhang, X. Fan, C. Yan, H. Li, Y. Zhu, X. Li, *et al.*, "Interfacial Microstructure and Properties of Carbon Fiber Composites Modified with Graphene Oxide," *ACS Applied Materials & Interfaces*, vol. 4, pp. 1543-1552, 2012/03/28 2012.
- [45] M. Tehrani, M. Safdari, A. Y. Boroujeni, Z. Razavi, S. W. Case, K. Dahmen, *et al.*, "Hybrid carbon fiber/carbon nanotube composites for structural damping applications," *Nanotechnology*, vol. 24, p. 155704, 2013.